ESC European Society of Cardiology

Cardiovascular Research (2021) **117**, 1746–1759
doi:10.1093/cvr/cvab024

NLRP3 inflammasome is a key driver of obesity-induced atrial arrhythmias

Larry Scott Jr [1], Anke C. Fender[2], Arnela Saljic[3], Luge Li[4], Xiaohui Chen [4], Xiaolei Wang [4], Dominik Linz [3,5,6], Jilu Lang[7], Mathias Hohl [8], Darragh Twomey [9], Thuy T. Pham[4], Rodrigo Diaz-Lankenau [4], Mihail G. Chelu [10], Markus Kamler [11], Mark L. Entman[4], George E. Taffet [4], Prashanthan Sanders [6], Dobromir Dobrev[2†], and Na Li [1,4,12*†]

[1]Department of Molecular Physiology and Biophysics, Baylor College of Medicine, Houston, TX, USA; [2]Institute of Pharmacology, West German Heart and Vascular Center, University Duisburg-Essen, Essen, Germany; [3]Laboratory of Cardiac Physiology, Department of Biomedical Sciences, University of Copenhagen, Copenhagen, Denmark; [4]Section of Cardiovascular Research, Department of Medicine, Baylor College of Medicine, Houston, TX, USA; [5]Department of Cardiology, Cardiovascular Research Institute Maastricht (CARIM), Maastricht University Medical Centre, Maastricht, The Netherlands; [6]Centre for Heart Rhythm Disorders, South Australian Health and Medical Research Institute, Royal Adelaide Hospital, University of Adelaide, Adelaide, Australia; [7]Department of Cardiac Center, The Seventh Affiliated Hospital, Sun Yat-Sen University, Shenzhen, China; [8]Department of Cardiology/Angiology, University-Clinic of Saarland, Internal Medicine III, Homburg/Saar, Germany; [9]James Cook University Hospital, Middlesbrough, UK; [10]Division of Cardiology, Department of Medicine, Baylor College of Medicine, Houston, TX, USA; [11]Department of Thoracic and Cardiovascular Surgery, West German Heart and Vascular Center, University Duisburg-Essen, Essen, Germany; and [12]Cardiovascular Research Institute, Baylor College of Medicine, Houston, TX, USA

Received 20 August 2020; revised 17 November 2020; editorial decision 14 January 2021; accepted 18 January 2021; online publish-ahead-of-print 1 February 2021

Time for primary review: 17 days

Aims Obesity, an established risk factor of atrial fibrillation (AF), is frequently associated with enhanced inflammatory response. However, whether inflammatory signaling is causally linked to AF pathogenesis in obesity remains elusive. We recently demonstrated that the constitutive activation of the 'NACHT, LRR, and PYD Domains-containing Protein 3' (NLRP3) inflammasome promotes AF susceptibility. In this study, we hypothesized that the NLRP3 inflammasome is a key driver of obesity-induced AF.

Methods and results Western blotting was performed to determine the level of NLRP3 inflammasome activation in atrial tissues of obese patients, sheep, and diet-induced obese (DIO) mice. The increased body weight in patients, sheep, and mice was associated with enhanced NLRP3-inflammasome activation. To determine whether NLRP3 contributes to the obesity-induced atrial arrhythmogenesis, wild-type (WT) and NLRP3 homozygous knockout ($NLRP3^{-/-}$) mice were subjected to high-fat-diet (HFD) or normal chow (NC) for 10 weeks. Relative to NC-fed WT mice, HFD-fed WT mice were more susceptible to pacing-induced AF with longer AF duration. In contrast, HFD-fed $NLRP3^{-/-}$ mice were resistant to pacing-induced AF. Optical mapping in DIO mice revealed an arrhythmogenic substrate characterized by abbreviated refractoriness and action potential duration (APD), two key determinants of reentry-promoting electrical remodeling. Upregulation of ultra-rapid delayed-rectifier K^+-channel (Kv1.5) contributed to the shortening of atrial refractoriness. Increased profibrotic signaling and fibrosis along with abnormal Ca^{2+} release from sarcoplasmic reticulum (SR) accompanied atrial arrhythmogenesis in DIO mice. Conversely, genetic ablation of *Nlrp3* ($NLRP3^{-/-}$) in HFD-fed mice prevented the increases in Kv1.5 and the evolution of electrical remodeling, the upregulation of profibrotic genes, and abnormal SR Ca^{2+} release in DIO mice.

Conclusion These results demonstrate that the atrial NLRP3 inflammasome is a key driver of obesity-induced atrial arrhythmogenesis and establishes a mechanistic link between obesity-induced AF and NLRP3-inflammasome activation.

* Corresponding author. Tel: +1 713 798 2335, E-mail: nal@bcm.edu
† The last two authors contributed equally to the study and share senior authorship.

Graphical Abstract

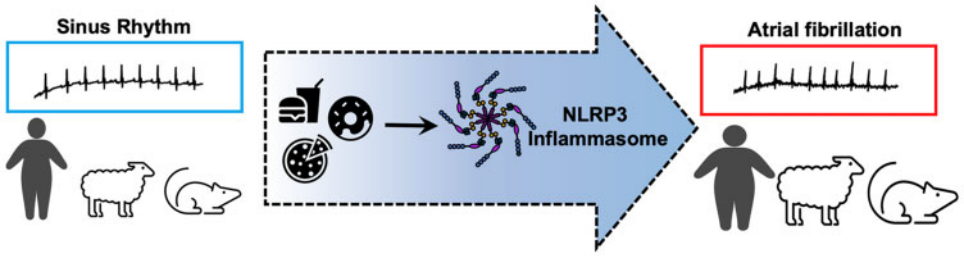

Keywords Atrial fibrillation • Obesity • NLRP3 inflammasome

1. Introduction

As the most common cardiac arrhythmia, the prevalence of atrial fibrillation (AF) is increasing worldwide and has become a significant public health burden.[1,2] Due to the variability of potential contributors and the limited understanding of the molecular mechanisms driving AF and its progression, the effect of current rhythm control strategies is limited in some patients.[3–5] Overweight and obesity have increasing prevalence, are established risk factors of AF and are associated with lower efficacy of rhythm control strategies.[6–10] Although diet-induced obese mice are prone to pacing-induced AF due to atrial remodeling,[11] the potential underlying mechanisms linking obesity and AF remain poorly understood.

Obesity is notably associated with sterile inflammation, which is another risk factor for AF.[12–18] It is well-known that the 'NACHT, LRR, and PYD Domains-containing Protein 3' (NLRP3) inflammasome, a well-established member of a family of NOD-like receptor (NLR) proteins, drives inflammation by producing proinflammatory cytokines such as interleukin (IL)-1β and IL-18.[19–21] We recently demonstrated that the activity of NLRP3 inflammasome is enhanced in atrial cardiomyocytes of AF patients.[22,23] Moreover, constitutive activation of NLRP3 exclusively in cardiomyocytes promotes atrial electrical remodeling by enhancing the expression and function of ultra-rapid outward K^+ current (I_{Kur}), which abbreviates the atrial action potential and promotes reentry, thereby increasing the susceptibility to AF in a genetic murine model.[23,24] Although the NLRP3 inflammasome is more active in adipose tissue of a mouse obesity model and in atrial tissues of patients with diabetes,[25,26] it is unknown whether obesity enhances the NLRP3 inflammasome in the atria, thereby promoting AF development.

In this study, we tested the hypothesis that the NLRP3 inflammasome is a key driver of obesity-induced AF. Our data show that the NLRP3-inflammasome is more active in atrial tissue of obese patients and obese sheep. Additionally, a diet-induced obesity mouse model developed a pro-arrhythmic substrate for AF, along with enhanced activity of the atrial NLRP3 inflammasome. Genetic inhibition of NLRP3 activity in mice prevented inducible AF, the development of the reentry-promoting substrate and the evolution of abnormal diastolic Ca^{2+} leak from the sarcoplasmic reticulum (SR) without correcting the obesity. These findings position the atrial NLRP3 inflammasome as a key driver of obesity-induced atrial arrhythmogenesis.

2. Methods

For detailed methods, see Supplementary material online.

2.1 Human atrial samples

The right atrial appendage (RAA) samples were collected from patients undergoing routine open-heart surgery for coronary bypass grafting and/or valve replacement (*Table 1* and Supplementary material online, *Figure S1*). All available RA-appendages were used consecutively; RA-appendages were not available from the following types of procedures: emergency surgery, off-pump and re-do procedures, or cases for which the surgeon judged that RA-sampling would excessively complicate the surgical procedure. Tissue samples were collected immediately prior to atrial cannulation for extracorporeal circulatory bypass, stored in Tyrode solution and transferred to the laboratory for freezing in liquid nitrogen. Patients with a previous history of AF, having left ventricular ejection fraction (LVEF) <40%, and those taking antiarrhythmic drugs were excluded. Patients were retrospectively classified as obese (Ob) if body mass index (BMI) was >30 and as control (Ctl) if BMI was <28. Targeted protein biochemistry (western blot, WB) of selected proteins was performed in each group as indicated. The STROBE check list used for this sub-study was provided in the Supplementary material online. Each patient gave written informed consent. All experimental protocols were approved by the Human Ethics Committee of the Medical Faculty of the University Duisburg-Essen (approval number AZ: 12-5268-BO) and were performed in accordance with the Declaration of Helsinki. Patient demographics and characteristics are listed in *Table 1*.

2.2 Sheep model of obesity

To evaluate the NLRP3-inflammasome activity in a pre-clinical large animal model of obesity, the atrial samples from a previously-established obese sheep model were used.[27] Briefly, eight sheep were fed ad libitum calorie-dense diet over 40 weeks to induce excessive weight gain, and the obese state was sustained for an additional 40 weeks. Eight lean, weight-controlled, and aged-matched sheep served as controls. The

Table 1 Patient characteristics

Characteristics	Ctl (non-obese)	Obese
Patients, *n*	6	9
Male gender, *n* (%)	4 (80)	6 (67)
Age (years), mean±SD	73 ± 6	71 ± 5
BMI (kg/m^2), mean±SD	25 ± 1	34 ± 2*
CAD, *n* (%)	0 (0)	4 (44)
AVD/MVD, *n* (%)	2 (33)	3 (33)
CAD+AVD/MVD, *n* (%)	4 (67)	2 (22)
Hypertension, *n* (%)	5 (83)	5 (55)
Hyperlipidemia, *n* (%)	3 (50)	8 (89)*
LA diameter (mm), mean±SD	47 ± 1	45 ± 8
LVEF (%), mean±SD[a]	60 ± 6[a]	56 ± 9[a]
Oral antidiabetic drugs, *n* (%)[b]	0 (0)	8 (89)*
Insulin, *n* (%)	0 (0)	8 (89)*
ACEI/ARB, *n* (%)	5 (83)	6 (67)
Beta blockers, *n* (%)	1 (17)	6 (67)
Calcium channel blockers, *n* (%)	0 (0)	1 (11)
Digitalis glycosides, *n* (%)	0 (0)	0 (0)
Diuretics, *n* (%)	1 (17)	5 (55)
Lipid-lowering drugs, *n* (%)	3 (50)	7 (78)
Oral anticoagulants, *n* (%)	0 (0)	0 (0)
Nitrates, *n* (%)	0 (0)	0 (0)
Platelet inhibitors, *n* (%)	3 (50)	8 (89)
CRP (mg/dL), mean±SD	0.75 ± 0.6	0.67 ± 0.52
Leucocytes (/nL), mean±SD	7.8 ± 1.4	8.7 ± 2.6

ACEI, angiotensin converting enzyme inhibitors; ARB, angiotensin receptor blockers; AVD, aortic valve disease; BMI, body mass index; CAD, coronary artery disease; CRP, C-reactive protein; LA, left atrial; LV, left ventricular; MI, myocardial infarction; MVD, mitral valve disease; SD, standard deviation.
*$P < 0.05$ determined by Wilcoxon rank sum test for continuous variables, and Fisher's exact test for categorical values.
[a]Data missing from $n = 2$ Control and $n = 4$ Obese patients.
[b]Metformin ($n = 3$), Sitagliptin ($n = 3$), Glibenclamide ($n = 1$), Dapagliflozin ($n = 1$).

animal research ethics committees of the University of Adelaide and the South Australian Health and Medical Research Institute, Adelaide, Australia, which adhere to the National Health and Medical Research Council of Australia Guidelines for the Care and Use of Animals for Research Purposes, approved the study. The investigation involving the use of animals conformed to the guidelines from Directive 2010/63/EU of the European Parliament on the protection of animals used for scientific purposes and the National Institutes of Health (NIH) Guide for the Care and Use of Laboratory Animals. General anaesthesia was used for all procedures. Diazepam (0.4 mg/kg, i.p) was administered prior to induction with ketamine (5 mg/kg, i.p). Inhalation of 2.5% isoflurane with O_2 (4 L/min) was used for maintenance. Non-invasive blood pressure, heart rate, pulse oximetry, and end-tidal CO_2 were continuously monitored. Inducibility of AF was determined using a burst pacing protocol in the left atrial appendage, which was performed as a terminal study. Twenty impulses were delivered at the lowest cycle length with 1:1 atrial capture. An episode was defined as irregular atrial activity lasting ≥2 s. This protocol was repeated five times and the number of episodes and total duration were recorded. Sustained AF was defined as an episode lasting >10 min. In the event of sustained AF, no further testing was performed. At study completion, euthanasia was performed by bilateral thoracotomy while the sheep was under a surgical plane of anaesthesia. Heart was removed and the right atrial appendage was isolated, and flash frozen in liquid N_2. NLRP3-inflammasome activation was assessed by immunoblot of atrial whole-tissue lysate.

2.3 Diet-induced obesity mouse model

Experiments with mice were approved by the Institutional Animal Care and Use Committee (IACUC) at Baylor College of Medicine (BCM). *In vivo* experiments and animal management procedures were conducted in accordance with the NIH Guide for Care and Use of Laboratory Animals.[28] To investigate the role of NLRP3 in obesity-induced AF, NLRP3 homozygous knockout mice (NLRP3$^{-/-}$) were purchased from the Jackson Laboratory (017969) and backcrossed to C57BL6/J for more than six generations.[29] Age- and gender-matched C57BL6/J wild-type (WT) and NLRP3$^{-/-}$ mice were subjected to a high-fat-diet (HFD) feeding to induce obesity.[30] Starting at the age of 6 weeks, WT and NLRP3$^{-/-}$ mice were fed with either normal chow (NC) or HFD (60%KCal fat; Research Diets D12492) for 10 weeks. Body weight (BW) was measured weekly in all 4 groups of mice: (i) WT+NC, (ii) WT+HFD, (iii) NLRP3$^{-/-}$+NC, and (iv) NLRP3$^{-/-}$+HFD. In cases when anaesthesia was required, mice were anaesthetized by inhaling 2% isoflurane (Henry Schein Animal Health, USA) in 100% oxygen (0.8–1.2 L/min) for 10–60 min depending on the procedures described below. Euthanasia was performed by cervical disarticulation while the mice were under a surgical plane of anaesthesia or after CO_2 induced unconsciousness.

2.4 Echocardiography

To characterize systolic cardiac function, echocardiography was performed under general anaesthesia (inhalation of 2% isoflurane in 100% O_2, 0.8–1.2 L/min) using VisualSonics Vevo 2100 Ultrasound at baseline and 10 weeks timepoints.[31]

2.5 Programmed intracardiac stimulation (PIS)

PIS was performed to induce AF as described previously.[23] Briefly, a 1.1 F octapolar catheter (EPR-100, Millar Instruments), inserted into the heart via the right jugular vein, was used to record atrial and ventricular intracardiac electrograms simultaneously. Bipolar right atrial pacing was administered via an external stimulator (STG-3008, MultiChannel Systems). An overdriving pacing protocol was applied for three times to induce AF for three times. Only mice that exhibited pacing-induced AF for longer than 2 seconds for at least 2 of 3 pacing protocols were considered AF positive. The average of the maximum duration of inducible AF was compared among WT+NC, WT+HFD, NLRP3$^{-/-}$+NC, and NLRP3$^{-/-}$+HFD groups.

2.6 Optical mapping

Optical mapping was performed as previously described.[23] Briefly, hearts were dissected and cannulated via the aorta and retrograde perfused and superfused with Tyrode's solution (2–5 mL/min). To load hearts with the voltage-sensitive dye, di4-ANEPPS (Invitrogen, 0.1 μmol/L, 1 mL) was slowly injected into a drug-port over 10 min period. Afterwards, blebbistatin (Sigma–Alrich, 6.8 μmol/L, 0.1 mL) was delivered to heart via the drug-port to eliminate motional artifacts. The emitted fluorescence V_m-signal was long-passed (>700nm) and acquired via MiCAM CMOS camera (SciMedia, USA) at the sampling rate of 1 kHz and pixel size of 100 μm/pixel. Right atrial pacing and surface ECG was recorded by PowerLab 26 T stimulator (AD Instruments, Australia).

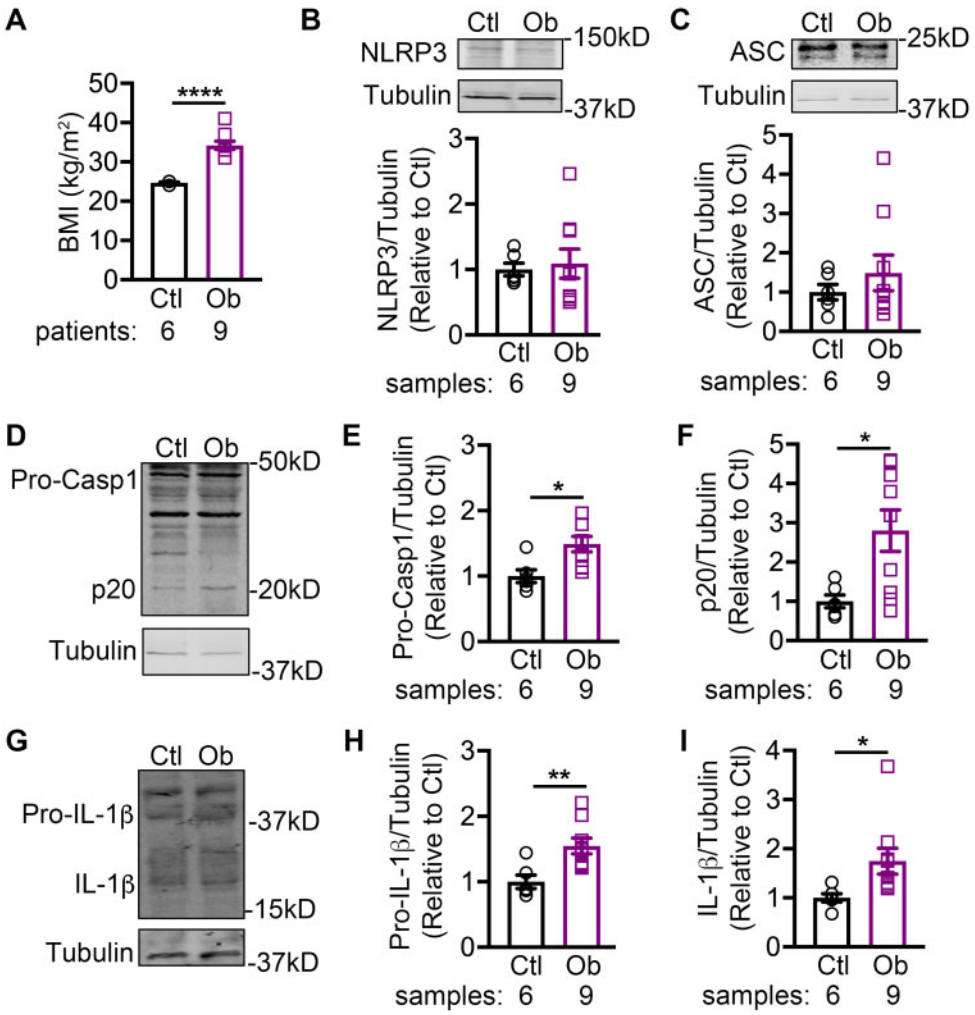

Figure 1 NLRP3 inflammasome correlates with increased body weight in patients. (*A*) Quantification of BMI in non-obese control (Ctl) and obese (Ob) patients. Representative western blots and quantification of NLRP3 (*B*) and ASC (*C*) in atrial tissues of patients. Representative western blots (*D*) and quantification of pro-caspase-1 (Pro-Casp1, *E*), and active caspase-1 (p20, *F*) in atrial tissues of patients. Representative western blots (*G*) and quantification of pro-IL-1β (*H*), and mature IL-1β (*I*) in atrial tissues of patients. $^{*}P < 0.05$, $^{**}P < 0.01$ using Student's *t*-test.

Atrial-effective-refractory period (AERP) was assessed with S1-S2-pacing at a CL of 100 ms.

A 5 ms pulse width and 5 V pulse amplitude were applied. Mapping results were analysed by ElectroMap, an established open-source software.[32] For 10 Hz pacing, activation maps were generated based on the depolarization midpoint value. Conduction velocity (CV) was calculated by multi-vector method for entire right atrium (RA).[32,33] Action potential duration (APD) at 20%, 50%, 70%, and 90% repolarization was calculated for RA. For each value, the average of 10 consecutive beats at 10 Hz pacing were calculated for each mouse.

2.7 Ca^{2+} imaging

Atrial cardiomyocytes were isolated using established methods and stored in KB solution at room temperature.[23,34,35] Isolated atrial cardiomyocytes were loaded with Fluo-4-AM (2.5 μmol/L) at room temperature for 30 min before imaging. Confocal line scan imaging was applied to the healthy atrial cardiomyocytes that followed 1 Hz pacing. 1 mmol/L caffeine was applied to cells to assess the sarcoplasmic reticulum (SR) Ca^{2+} load. Ca^{2+}-spark frequency (CaSF) during diastole was calculated using SparkMaster.[36]

2.8 Statistical analysis

Numerical data were presented as the mean ± SEM (for animal studies) and mean ± SD (for human studies). Two-tailed Student's *t*-tests were used to compare data between two groups with normal distributed values. ANOVA with post hoc Sidak tests were used comparing normally distributed data with multiple comparisons. Kruskal–Wallis test with post hoc Dunn tests were used to compare nonparametric data with multiple comparisons. Fisher's exact test was used to compare categorical data. A *P*-value <0.05 was considered statistically significant.

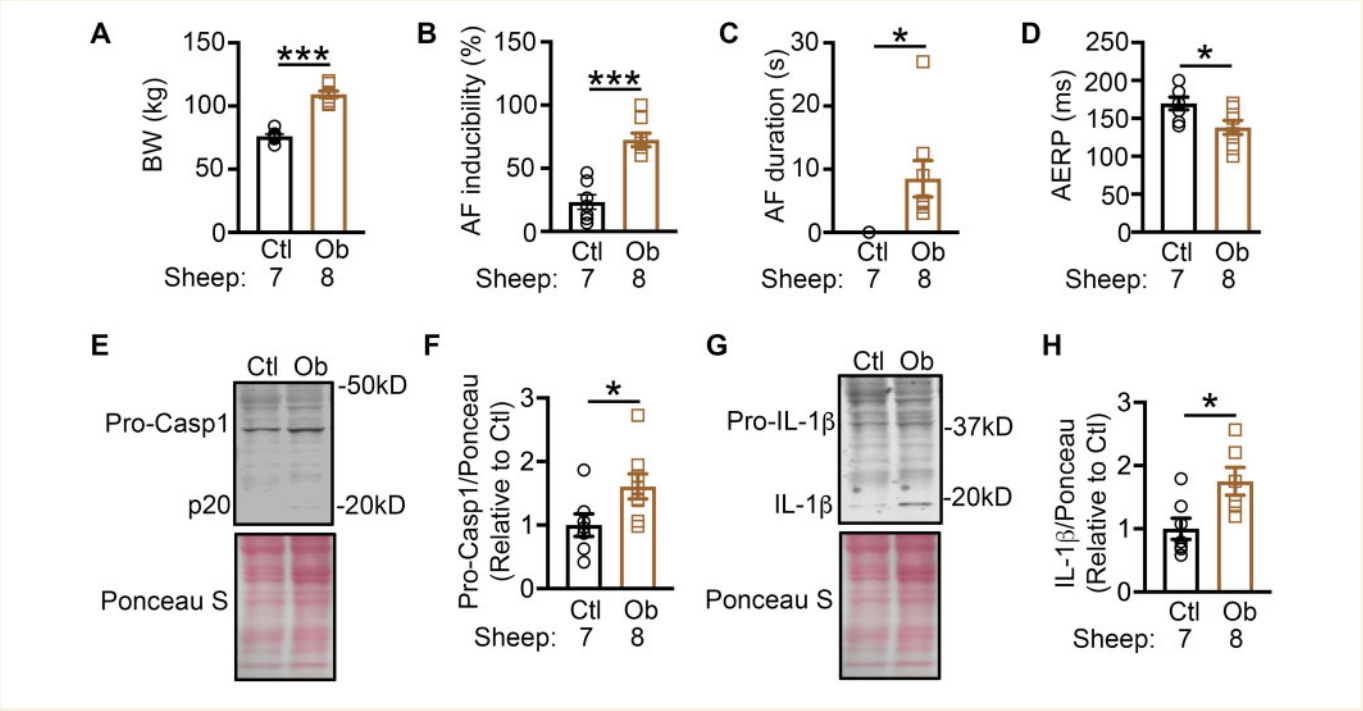

Figure 2 Enhanced NLRP3 inflammasome activity in atrial samples of obese sheep. Quantification of body weight (BW, *A*), AF inducibility (*B*), duration of the inducible AF (*C*), AERP (*D*) in lean control (Ctl) and obese (Ob) sheep. Representative western blots of Caspase-1 (*E*) and IL-1β (*G*) in Ctl and Ob sheep. Quantification of pro-Casp1 (*F*) and mature IL-1β (*H*) in Ctl and Ob sheep. *$P < 0.05$, ***$P < 0.001$ using Student's *t*-test.

3. Results

3.1 Atrial NLRP3-inflammasome activity correlates with body weight in both patients and sheep

To elucidate the association between obesity and the NLRP3-inflammasome activity in human atria, we utilized a cohort of human RAA samples collected from non-obese control patients and obese patients (*Table 1*). The body-mass index (BMI) was significantly higher in the obese patients (34 ± 2 kg/m^2) than in control patients (25 ± 1 kg/m^2, $P < 0.001$, *Figure 1A*). Western blots revealed that the levels of precursor caspase-1 (Pro-Casp1, *Figure 1D and E*), cleaved caspase-1 (p20, *Figure 1D and F*), precursor IL-1β (*Figure 1G and H*), and mature IL-1β (*Figure 1G and I*), were all significantly increased in the obese patients compared to the non-obese control patients, despite the unchanged protein levels of NLRP3 (*Figure 1B*) and ASC (*Figure 1C*). These results suggest that 'triggering' (assembly and thus activation) but not 'priming' (increased transcription of the components) mechanisms contribute to the NLRP3-inflammasome activation with obesity.

Since co-morbidities and risk factors could confound the NLRP3-inflammasome activation in human atria, we confirmed our human results in atrial samples collected from a previously-established sheep model of obesity (*Figure 2A*).[23] Obese sheep showed a greater tendency to develop pacing-induced AF relative to lean sheep (*Figure 2B*). The duration of inducible-AF was also significantly increased in obese sheep compared to the lean sheep (*Figure 2C*), suggesting the presence of an obesity-related reentry-promoting substrate, which was associated with a shortening of the AERP (*Figure 2D*). As expected, the levels of Pro-Casp1 and mature IL-1β were higher in the RAA samples of obese compared to lean sheep (*Figure 2E–H*). These results validate that obesity or enhanced body weight promote atrial NLRP3-inflammasome activation.

3.2 Diet-induced obesity activates the NLRP3 inflammasome in mouse atria

To elucidate the role of NLRP3 in obesity-related atrial arrhythmogenesis, we established the diet-induced obese mouse model by subjecting WT and NLRP3$^{-/-}$ mice to NC and HFD, respectively. At the age of 6 weeks, there was no difference in baseline BW between the age-matched WT (22.0 ± 0.3g) and NLRP3$^{-/-}$ (21.4 ± 0.3g, $P = 0.954$) mice. About 10 weeks later, WT mice subjected to HFD (WT+HFD) gained more BW than WT mice that received NC (WT+NC) (37.4 ± 1.1g vs. 31.4 ± 0.6g, $P < 0.0001$, *Figure 3A*). The inguinal and epididymal white adipose tissue (iWAT, eWAT) were more abundant in WT+HFD mice vs. the WT+NC controls ($P < 0.05$, $P < 0.001$) (*Figure 3B*). Similarly, NLRP3$^{-/-}$ mice fed with HFD (NLRP3$^{-/-}$+HFD) also gained more weight (NLRP3$^{-/-}$+NC: 31.6 ± 0.9g vs. NLRP3$^{-/-}$+HFD: 38.2 ± 0.7g, $P < 0.001$) and accumulated more iWAT and eWAT compared to NC-fed NLRP3$^{-/-}$ mice (NLRP3$^{-/-}$+NC) (*Figure 3A and B*). Relative to baseline BW, the percentage weight gain in WT and NLRP3$^{-/-}$ mice after 10 weeks HFD feeding were similar (WT+HFD: 72.4 ± 2.0% vs. NLRP3$^{-/-}$+HFD: 77.3 ± 2.1%, Supplementary material online, *Figure S2*). The excessive accumulation of adipose tissue in HFD-treated mice further confirmed the development of diet-induced obesity in both WT and NLRP3$^{-/-}$ mice.

To determine whether the levels of glucose and insulin are altered after 10 weeks of HFD, glucose tolerance tests (GTT) and insulin tolerance tests (ITT) were performed. Similar to previous reports, glucose level during GTT was increased in WT+HFD mice compared to

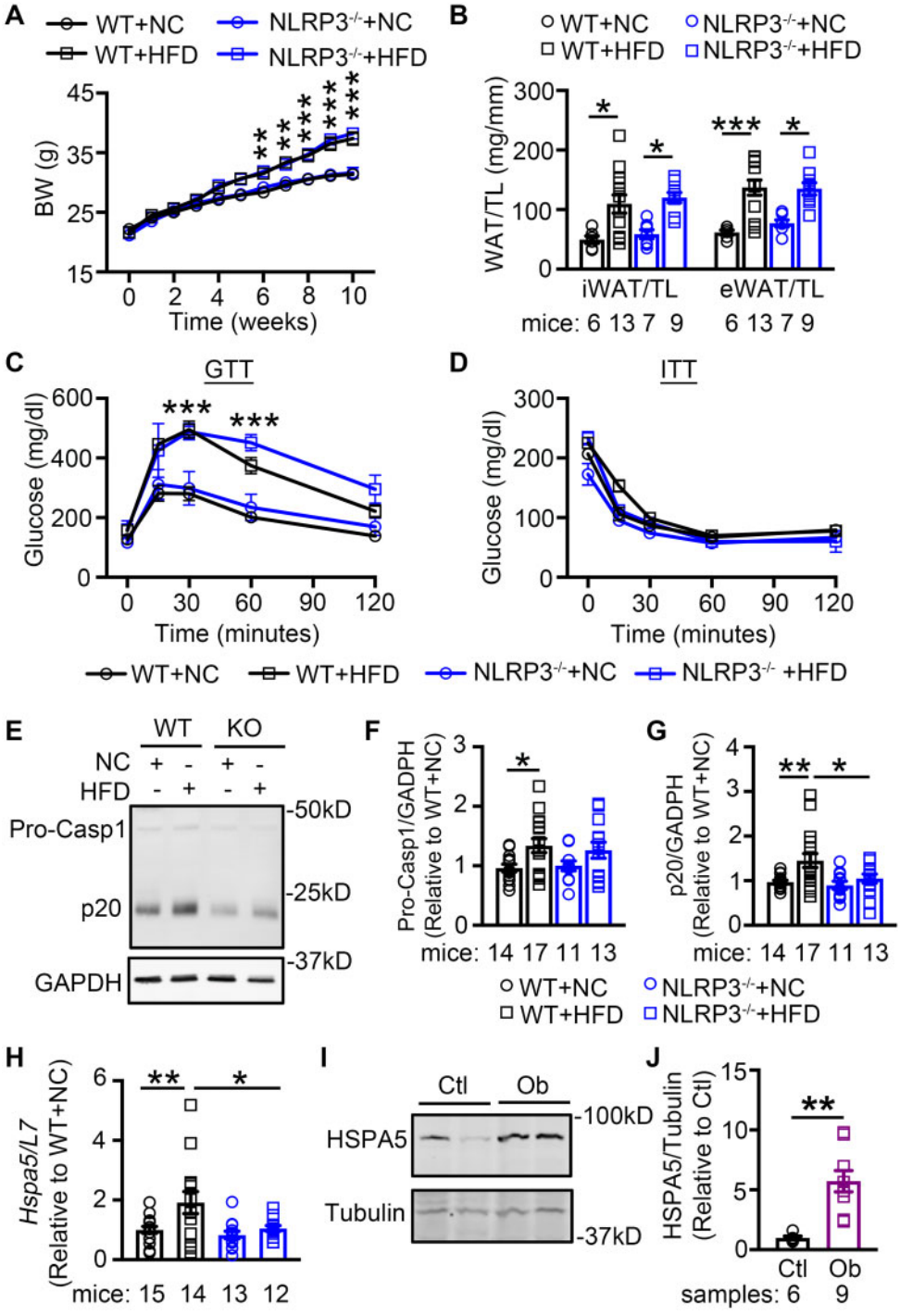

Figure 3 Diet-induced obesity promotes activation of NLRP3 inflammasome in atria. (*A*) Weekly body weight (BW) measurements in WT and NLRP3$^{-/-}$ mice fed with normal chow (NC) or high-fat-diet (HFD), respectively (N = 13 WT+NC, 19 WT+HFD, 12 NLRP3$^{-/-}$+NC, 17 NLRP3$^{-/-}$+HFD). (*B*) Quantification of iWAT and eWAT normalized to tibial length (TL) in WT and NLRP3$^{-/-}$ mice after 10 weeks' feeding of NC or HFD, respectively. (*C* and *D*) Plasma level of glucose during glucose-tolerance test (GTT, C) and insulin-tolerance test (ITT, *D*) in WT and NLRP3$^{-/-}$ mice after 10 weeks' feeding of NC or HFD, respectively (N = 9 WT+NC, 10 WT+HFD, 6 NLRP3$^{-/-}$+NC, 3 NLRP3$^{-/-}$+HFD). (*E*–*G*) Representative western blots (*E*) and quantification of Pro-Casp1 (*F*) and p20 (*G*) in atrial tissues of WT and NLRP3$^{-/-}$ mice after 10 weeks' feeding of NC or HFD. (*H*) mRNA levels of *Hspa5 in* atrial tissues of WT and NLRP3$^{-/-}$ mice after 10 weeks' feeding of NC or HFD, respectively. (*I* and *J*) Representative western blots and quantification of HSPA5 protein level in atrial tissues of non-obese control (Ctl) and obese (Ob) patients. *$P < 0.05$, **$P < 0.01$, ***$P < 0.001$ determined by Sidak test following one-way ANOVA.

WT+NC mice (*Figure 3C* and Supplementary material online, *Figure S3*). NLRP3$^{-/-}$+HFD mice also exhibited a higher glucose level than NLRP3$^{-/-}$+NC mice (*Figure 3C* and Supplementary material online, *Figure S3*). However, during the ITT, glucose clearance profiles were comparable among the tested groups (*Figure 3D*). These results suggest that 10 weeks HFD promoted the development of a pre-diabetic obese phenotype, and inhibition of NLRP3 did not impede the development of obesity and glucose intolerance associated with obesity.

To evaluate whether obesity activates the NLRP3 inflammasome in mouse atria, we measured the protein levels of Pro-Casp1 and activate p20 in atrial tissues harvested from the WT+NC, WT+HFD, NLRP3$^{-/-}$+NC, and NLRP3$^{-/-}$+HFD mice. We found that Pro-Casp1 and p20 (*Figure 3E–G*) were significantly increased in WT+HFD compared with the WT+NC mice, whereas the protein increases in Pro-Casp1 and p20 were absent in NLRP3$^{-/-}$+HFD compared to NLRP3$^{-/-}$+NC mice. To determine whether HFD led to systemic inflammation, we measured inflammatory markers in blood. The serum levels of IL-1β, IL-18, and the inflammatory marker C-reactive protein (CRP) were unchanged in mice that received HFD, compared to the mice that received NC (Supplementary material online, *Figure S4*). Similarly, the CRP and circulating leucocyte levels were comparable between non-obese control patients and obese patients (*Table 1*), indicative of the lack of systematic inflammatory response. These results suggest obesity caused an atrial-specific activation of the NLRP3-inflammasome in both our mouse and human samples.

Previous work has shown that saturated fatty acids can activate NLRP3 inflammasome via endoplasmic reticulum (ER) stress.[37] Since specific saturated fatty acids were enriched in the HFD, we sought to explore the potential involvement of ER stress in obesity-induced inflammasome activation in atria. To evaluate the levels of long-chain fatty acids in atrial tissues of the 4 groups of mice, we employed targeted metabolomics (Supplementary material online, *Figure S5A*). As expected, we found that the palmitic acid level was consistently elevated in HFD-treated WT and NLRP3$^{-/-}$ mice, compared with the NC-treated mice (Supplementary material online, *Figure S5B*). To assess whether ER stress is enhanced in HFD-fed mice, we evaluated the level of ER stress marker—*Hspa5* (encoding heat shock protein family A member 5, HSPA5) by qPCR. The level of *Hspa5* mRNA was significantly increased in WT+HFD mice ($P < 0.01$ vs. WT+NC) (*Figure 3H*). Similarly, the protein level of HSPA5 was markedly increased in atrial samples of obese patients ($P < 0.01$, *Figure 3I and J*). Genetic inhibition of NLRP3 attenuated the HFD-induced upregulation of HSPA5 (NLRP3$^{-/-}$+HFD vs. WT+HFD, $P < 0.05$, *Figure 3H*) pointing to a causative link. These results suggest that obesity is associated with markers of selective ER stress signaling that might be a trigger of obesity-related NLRP3-inflammasome activation.

3.3 NLRP3 inflammasome increases the susceptibility to obesity-related AF

To determine whether obesity affects cardiac electrophysiology, we measured the ECG parameters in all 4 groups of mice after 10 weeks feeding. PQ-, QRS-, and QTc-intervals, sinus node recover time (SNRT), and atrioventricular node effective refractory period (AVNERP) parameters were all comparable among 4 groups of mice (Supplementary material online, *Table S1*). Heart rate (HR) was faster in WT+HFD mice than in WT+NC mice ($P < 0.05$), possibly due to sympathetic overactivity associated with the obesity.[38,39] In contrast, HR was comparable between NLRP3$^{-/-}$+NC and NLRP3$^{-/-}$+HFD mice ($P = 0.112$).

To determine whether obese mice were more susceptible to inducible AF, rapid atrial pacing was performed to induce AF after 10 weeks feeding. We found that both WT+NC (18.8%, $n = 16$) and NLRP3$^{-/-}$+NC (16.7%, $n = 6$) mice had very low susceptibility to pacing-induced AF. However, compared to WT+NC mice, WT+HFD mice were much more susceptible to pacing-induced AF, with an incidence of 82.4% ($n = 17$, $P < 0.01$ vs. WT+NC). In contrast, the incidence of pacing-induced AF was reduced to 27.3% in NLRP3$^{-/-}$+HFD mice ($n = 11$, $P < 0.05$ vs. WT+HFD) (*Figure 4A and B*). Moreover, the maximum duration of AF episodes was significantly longer in WT+HFD mice (40.2 ± 13.3 ms) than in WT+NC (6.8 ± 4.2 ms, $P < 0.01$) and NLRP3$^{-/-}$+HFD mice (13.1 ± 10.3 ms, $P < 0.05$, *Figure 4C*). These results establish that diet-induced obesity increases AF susceptibility, which is strongly attenuated by genetic NLRP3 inhibition.

To exclude that the increase in AF susceptibility in obese mice is due to ventricular dysfunction, we assessed the ventricular structure and contractility using echocardiography before and after 10 weeks feeding. We found that ejection fraction (EF%), left ventricular diameters (end-systolic diameter and end-diastolic diameter), and thickness of the left-ventricular-posterior-wall (LVPW) were comparable among all 4 groups of mice at both timepoints (*Figure 4D–G*; Supplementary material online, *Table S2* and *Figure S6*). Thus, the increased AF inducibility in the diet-induced obesity mice is primarily due to atrial remodeling in the absence of left ventricular dysfunction.

3.4 NLRP3 inflammasome creates a reentry substrate for obesity-related AF

To delineate the pro-arrhythmic components of the obesity-related AF-promoting substrate, we performed optical mapping to assess the CV and AERP. We revealed that CV in RA at 10 Hz pacing (pacing cycle length 100 ms) was comparable between HFD-fed WT and NLRP3$^{-/-}$ mice, despite the slightly decreased CV in NC-fed NLRP3$^{-/-}$ mice compared to NC-fed WT mice ($P = 0.064$, *Figure 5A and B*). AERP was significantly shorter in WT+HFD compared to WT+NC mice (9.8 ± 0.6 ms vs. 17 ± 1.6 ms, $P < 0.01$, *Figure 5C*), pointing to the evolution of a reentry-promoting atrial substrate. APD_{90} was shorter in WT+HFD mice compared to other mouse groups, while APD_{20}, APD_{50}, and APD_{70} were similar among all groups (*Figure 5D*). NLRP3 deficiency eliminated the differences between NLRP3$^{-/-}$+NC and NLRP3$^{-/-}$+HFD mice (AERP: 14.1 ± 2.3 ms vs. 13.3 ± 1.5 ms, $P = 0.385$, *Figure 5C*), indicating that the inhibition of NLRP3 prevented the obesity-induced shortening of AERP and APD_{90}.

To further delineate the potential molecular mechanisms underlying the shortening of AERP and APD, we evaluated the expression of major ion-channel subunits including voltage-dependent Na^+-channel (Nav1.5), α-subunit of L-type Ca^{2+}-channel (Cav1.2), and ultra-rapid delayed-rectifier K^+-channel (Kv1.5) in atrial tissue of obese patients and obese mice. We found that the protein levels of Nav1.5 and Cav1.2 were comparable between obese patients and control patients and NC- and HFD-fed WT and NLRP3$^{-/-}$ mice (Supplementary material online, *Figure S7A–D*). We have previously shown that constitutive activation of NLRP3 in a cardiomyocyte-specific knockin mouse model reduces AERP by enhancing the expression and function of Kv1.5. Accordingly, *Kcna5* (encoding Kv1.5) mRNA and Kv1.5 protein levels were upregulated in WT+HFD compared to WT+NC mice ($P < 0.05$, *Figure 5E and F*). Consistent with the correction in AERP, *Kcna5* mRNA and Kv1.5 protein

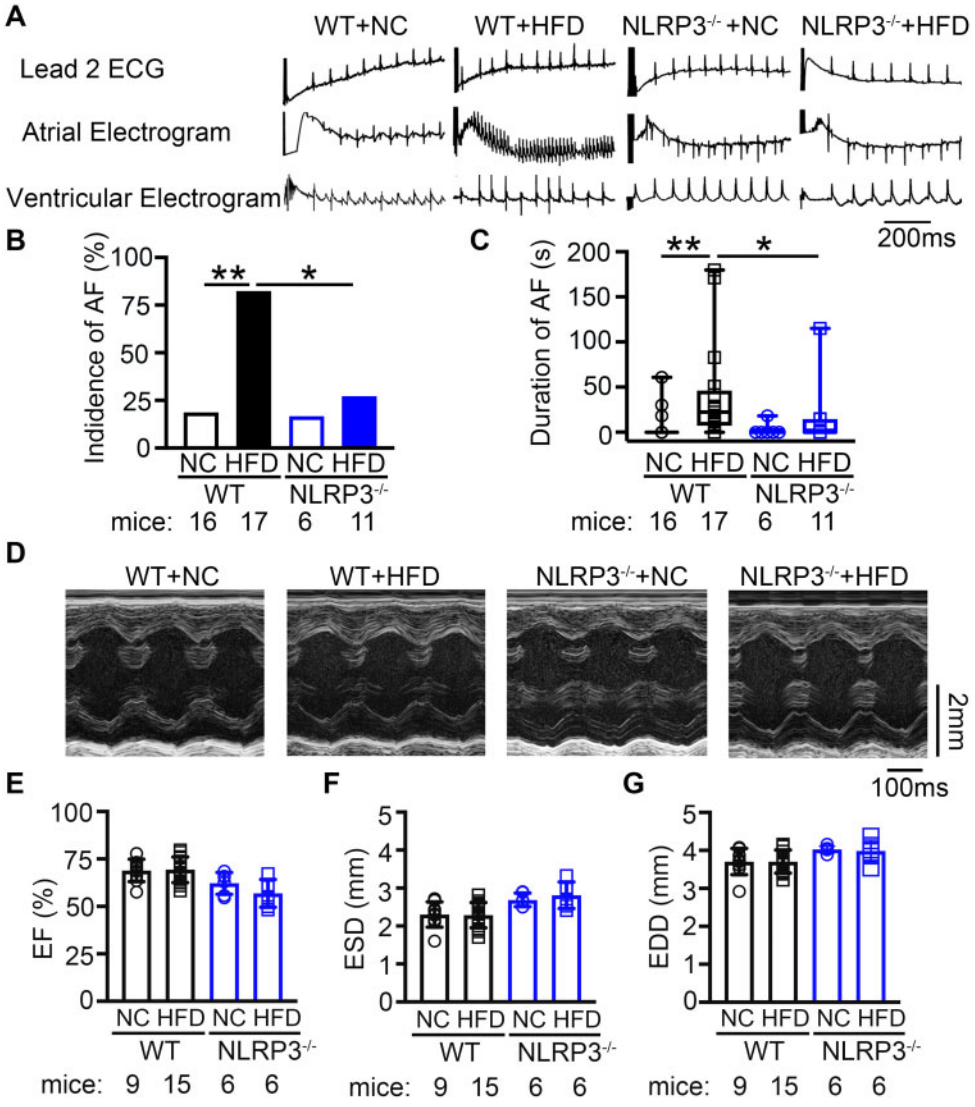

Figure 4 NLRP3 inflammasome upregulation increases the susceptibility to obesity-related AF inducibility. (*A*) Representative recordings of lead-2 surface ECG and intracardiac electrograms in WT and NLRP3$^{-/-}$ mice after 10 weeks' feeding of NC or HFD, respectively. (*B*) The incidence of pacing-induced reproducible AF. *$P < 0.05$ determined by Fisher's exact test. (*C*) The maximum duration of pacing-induced AF. *$P < 0.05$, **$P < 0.01$ determined by Kruskal–Wallis test. (*C*) Representative M-mode echocardiograph. (*D–F*) Summary of ejection fraction (EF%, *D*), end-systolic diameter (ESD, *E*), and end-diastolic diameter (EDD, *F*) of WT and NLRP3$^{-/-}$ mice after 10 weeks' feeding of NC or HFD, respectively. $P > 0.05$ determined by Sidak test following one-way ANOVA.

levels were normalized in NLRP3$^{-/-}$+HFD mice ($P < 0.01$, $P < 0.05$ vs. WT+HFD, *Figure 5E and F*). Moreover, the Kv1.5 protein levels were strongly increased in the atria of obese patients, compared to control patients, phenocopying WT+HFD mice ($P < 0.05$, *Figure 5G*). These results position the NLRP3-mediated Kv1.5 upregulation as a major contributor to electrical remodeling in obesity-induced AF.

Previous work showed that activation of NLRP3 could cause hypertrophy and fibrosis in the heart.[23] To evaluate whether atria are dilated in obese mice, echography was performed to assess the LA dimensions.[40,41] The superoinferior, anteroposterior, and mediolateral dimensions, and LA volume were comparable among 4 groups of mice (Supplementary material online, *Table S3* and *Figure S8*). This result suggests that atrial dilation is not a contributing factor to the development of the AF substrate in HFD fed mice. We then assessed whether fibrosis potentially contributes to the reentry-promoting atrial substrate in obesity. We found that the protein levels of collagen-1 (COL1A) and α-smooth muscle actin (α-SMA) were higher in obese than in control patients (*Figure 6A–C*), whereas fibronectin-1 (FN1), vimentin, and matrix metallopeptidase 9 (MMP9) were similar in both group (*Figure 6D and E*). HFD-fed WT similarly showed more atrial fibrosis based on histology (*Figure 6F*) and increases in mRNA levels of profibrotic α-SMA (*Acta2*), vimentin (*Vim*), and fibronectin (*Fn1*), phenocopying the structural changes in atria of obese patients (*Figure 6G*). Moreover, HFD-fed NLRP3$^{-/-}$ mice showed less fibrosis (*Figure 6F*) and normalized mRNA levels of *Acta2, Vim*, and *Fn1*, validating the causal relationship between NLRP3 and profibrotic atrial remodeling in obesity (*Figure 6G*).

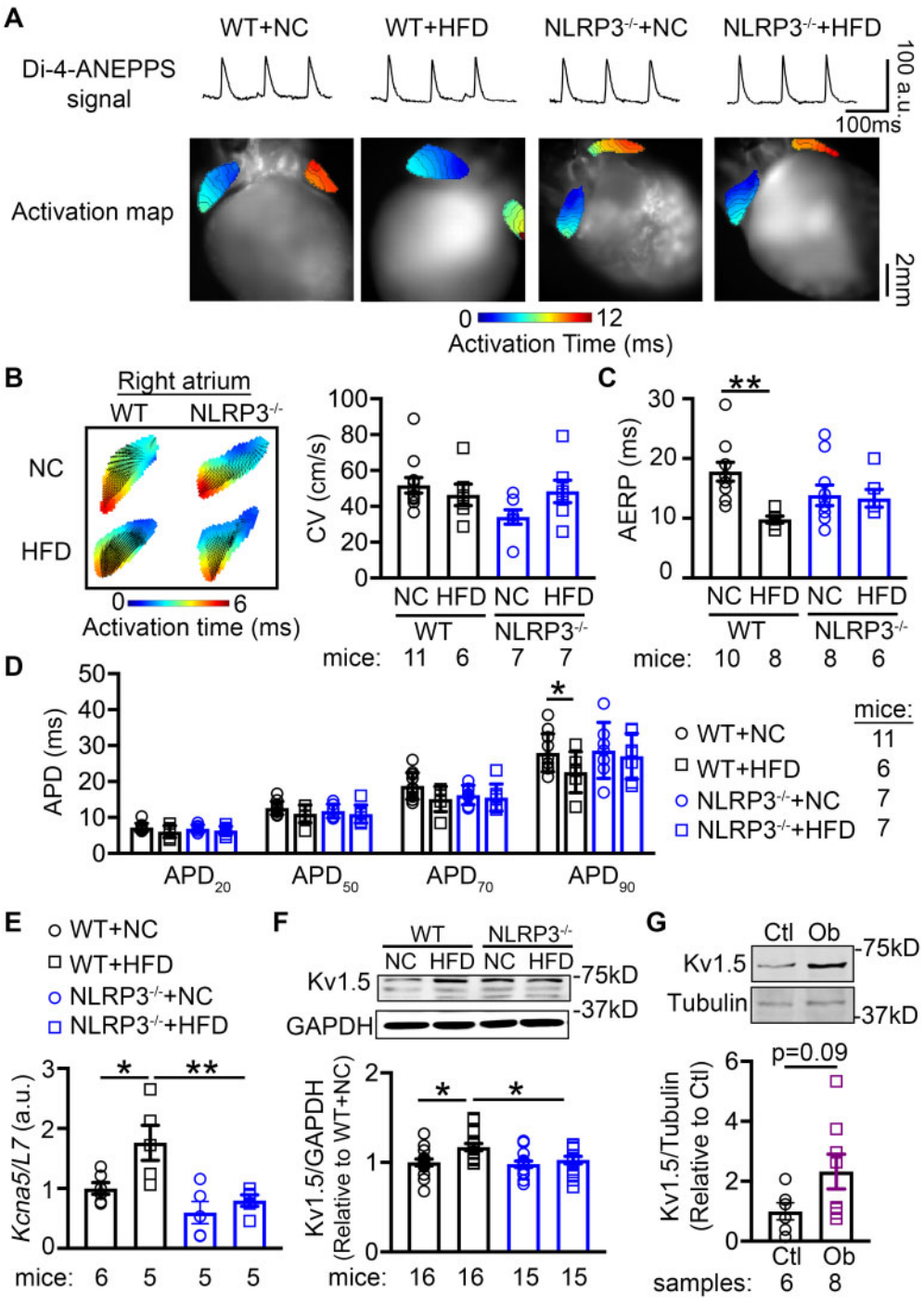

Figure 5 NLRP3 inflammasome contributes to the evolution of a pro-arrhythmic substrate for AF. (*A*) Representative optical di-4-ANEPPS signal and activation maps from optical mapping study. (*B*) Summary of conduction velocity (CV) in right atrium, and (*C*) atrial effective refractory period (AERP) in atria of WT and NLRP3$^{-/-}$ mice after 10 weeks' feeding of NC or HFD, respectively. (*D*) Action potential duration (APD) at 20%, 50%, 70%, and 90% repolarization in right atrium. The relative level of *Kcna5* mRNA (*E*) and Kv1.5 protein (*F*) in atria of WT and NLRP3$^{-/-}$ mice after 10 weeks' feeding of NC or HFD, respectively. $^{*}P < 0.05$, $^{**}P < 0.01$ determined by Sidak test following one-way ANOVA. (*G*) Representative western blots and quantification of Kv1.5 protein level in atrial tissues of non-obese control (Ctl) and obese (Ob) patients. $P = 0.09$ determined by Student's *t*-test.

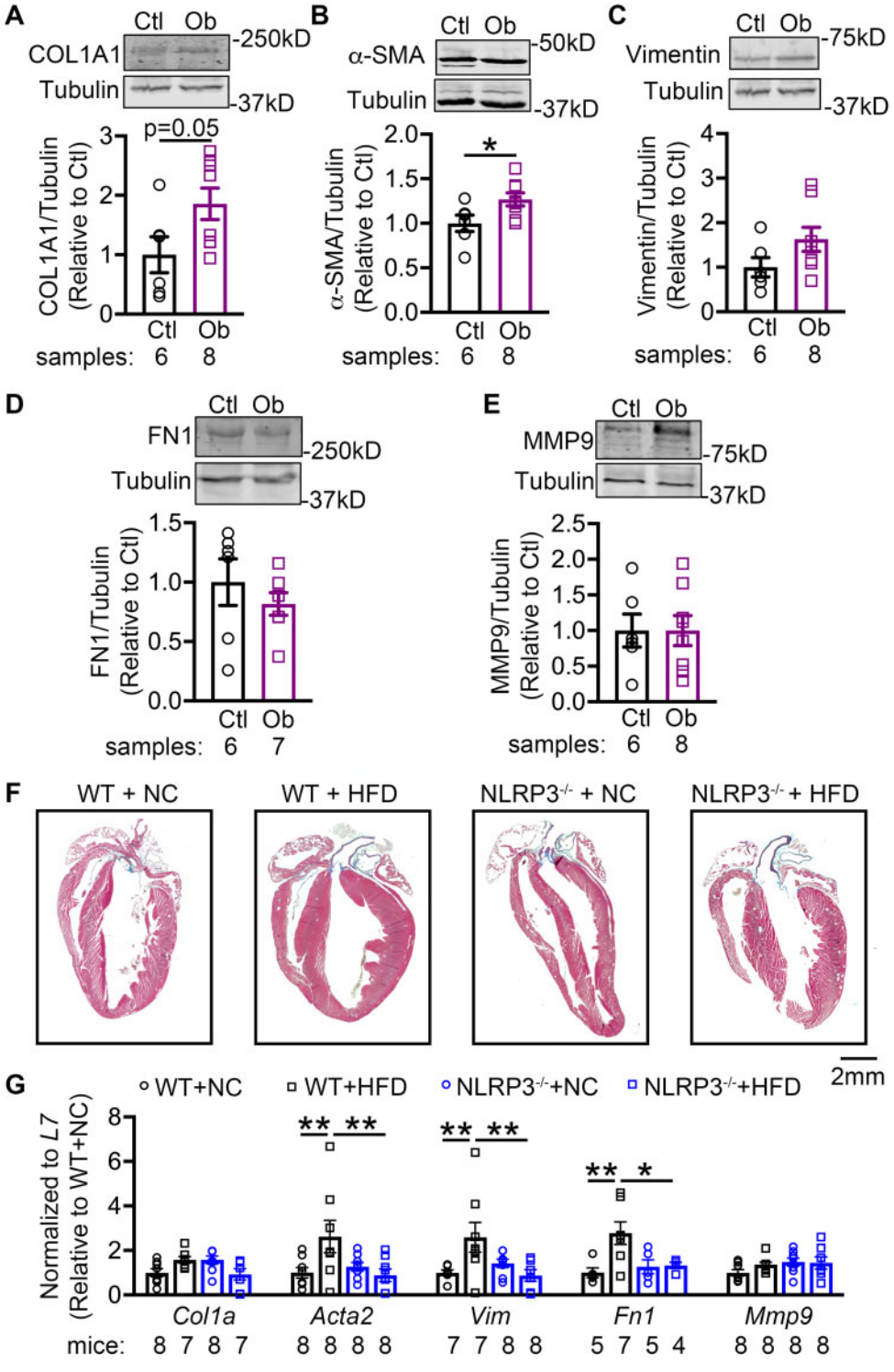

Figure 6 NLRP3 promotes atrial fibrosis in obesity-related AF. Representative western blots and quantification of collagen 1 A (COL1A, *A*), alpha-smooth muscle actin (α-SMA, *B*), vimentin (*C*), fibronectin-1 (FN1, *D*), and matrix metallopeptidase 9 (MMP9, *E*) protein in atrial tissues of non-obese control (Ctl) and obese (Ob) patients. $^{*}P < 0.05$ determined by Student's *t*-test. (*F*) Representative Masson's trichrome staining in whole hearts of WT and NLRP3$^{-/-}$ mice after 10 weeks' feeding of NC or HFD, respectively. (*G*) Relative levels of *Col1a, Acta2, Vim, Fn1*, and *Mmp9* in atrial tissues of WT and NLRP3$^{-/-}$ mice after 10 weeks' feeding of NC or HFD, respectively. $^{*}P < 0.05$, $^{**}P < 0.01$ determined by Sidak test following one-way ANOVA.

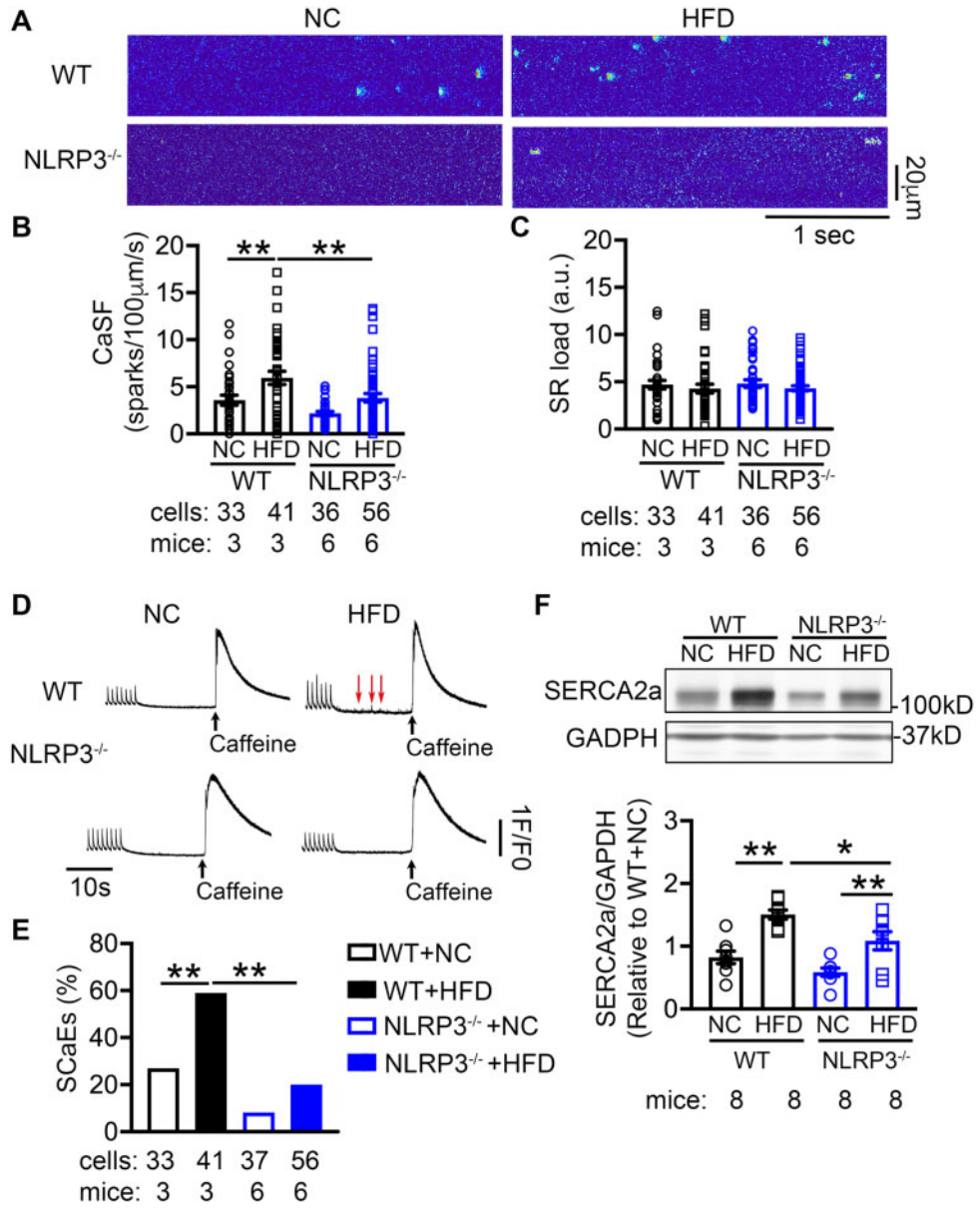

Figure 7 NLRP3 promotes aberrant sarcoplasmic reticulum (SR) Ca^{2+} release in obesity-related AF. (*A*) Representative Ca^{2+}-spark recordings, (*B*) quantification of Ca^{2+}-spark frequency (CaSF), and (*C*) estimation of SR Ca^{2+}-load in atrial cardiomyocytes of WT and NLRP3$^{-/-}$ mice after 10 weeks' feeding of NC or HFD, respectively. $^{**}P < 0.01$ determined by Sidak test following one-way ANOVA. (*D*) Representative recordings of pacing-induced Ca^{2+}-transients (CaT), followed by spontaneous Ca^{2+}-release events (SCaEs) and caffeine (10 mmol/L)-induced SR Ca^{2+} release as an index of SR Ca^{2+}-load. (*E*) Quantification of SCaEs in atrial cardiomyocytes, $^{**}P < 0.01$ determined by Student's *t*-test. (*F*) representative western blots and quantification of SERCA2a protein levels in atrial tissues of WT and NLRP3$^{-/-}$ mice after 10 weeks' feeding of NC or HFD, respectively. $^{*}P < 0.05$, $^{**}P < 0.01$ determined by Sidak test following one-way ANOVA.

3.5 NLRP3 inflammasome promotes aberrant diastolic Ca^{2+} leak in obesity-related AF

Abnormal Ca^{2+} release via sarcoplasmic reticulum (SR) is an important cellular mechanism contributing to both ectopic (triggered) activity and reentry.[42] To determine whether obesity promotes spontaneous SR Ca^{2+}-release events (SCaEs), we assessed Ca^{2+} sparks and Ca^{2+} transients (CaTs) in atrial cardiomyocytes isolated from the 4 groups of mice. Compared with the WT+NC mice, Ca^{2+}-spark frequency (CaSF) was increased in WT+HFD mice (3.6 ± 0.5 vs. 5.9 ± 0.7 sparks/100 μm/s, $P < 0.01$, *Figure 7A and B*), while SR Ca^{2+}-load (*Figure 7C and D*), amplitude and rate-constant of electrically stimulated CaTs (K_{CaT}) and caffeine-induced CaT (K_{Caff}) were unchanged (Supplementary material online, *Figure S9A–C*). SCaEs were more frequently observed in WT+HFD than WT+NC mice ($P < 0.01$, *Figure 7D and E*). Most important, NLRP3$^{-/-}$+HFD mice exhibited less CaSF (3.8 ± 0.4 sparks/100 μm/

s, $P < 0.01$, *Figure 7A and B*) and SCaEs ($P < 0.01$, *Figure 7D and E*) than WT+HFD mice, while SR Ca^{2+}-load, amplitude, K_{CaT}, and K_{Caff} remained comparable. Previous work showed that NLRP3 could activate CaMKII thereby increasing S2814-phosphorylation of RyR2 and Ca^{2+}-spark frequency.[22] However, the protein levels of total and T287-autophophorylated (activated) CaMKII were comparable between obese vs. control patients and NC- vs. HFD-fed WT and $NLRP3^{-/-}$ mice. Additionally, there was no difference in phosphorylated RyR2-S2814, and PLB-T17 among the 4 mouse groups (Supplementary material online, *Figure S9D–G*). Thus, CaMKII does not appear to be a key upstream regulator of atrial NLRP3 in this model of obesity. Moreover, the levels of phosphorylated RyR2-S2808 (PKA-phosphorylation site)[43] and phosphorylated RyR2-S2367 (SPEG-phosphorylation site),[44] and other major RyR2-regulatory and Ca^{2+}-handling proteins (calsequestrin-2, junctophilin-2, and Na^{+}/Ca^{2+} exchanger-1) were comparable among the 4 groups of mice (Supplementary material online, *Figure S10*), with the exception of sarcoplasmic/endoplasmic reticulum Ca^{2+} ATPase-2a (SERCA2a). We found that the SERCA2a protein was increased by 50% in WT+HFD mice than in WT+NC mice ($P < 0.01$, *Figure 7F*), which was attenuated in $NLRP3^{-/-}$+HFD mice ($P < 0.05$, *Figure 7F*). These results suggest that more Ca^{2+} could be sequestered into SR via SERCA2a in atrial myocytes of HFD fed mice, which could contribute to SR Ca^{2+} leak. Overall, these data indicate that obesity-induced NLRP3 activation produces abnormal Ca^{2+} handling and SR Ca^{2+} leak that may contribute to both AF-promoting triggered activity and reentry.

4. Discussion

Obesity and inflammation are two independent risk factors of AF. Obesity is frequently associated with enhanced inflammatory responses. However, whether and how inflammatory signaling mediates atrial arrhythmogenesis in the context of obesity is largely unknown. In this study, we report that: (i) activity of the NLRP3 inflammasome increases with BMI elevation in patients; (ii) HFD-induced obesity promotes NLRP3-inflammasome activation in both sheep and mice; (iii) the obesity-induced enhancement of AF susceptibility is driven by the NLRP3 inflammasome; and (iv) selective inhibition of NLRP3 prevents the development of the reentry substrate and abnormal Ca^{2+} release in obese mice, thereby preventing obesity-related AF. Our data also point to fatty acid-induced ER stress as a potential trigger of obesity-associated NLRP3-inflammasome activation, a hypothesis that needs direct testing in subsequent work.

Obesity is a modifiable risk factor of AF.[9,45] BMI correlates significantly with a higher risk of AF development.[46] It is known that greater BMI is associated with increased AF burden and an enhanced incidence of post-operative AF occurrence,[7,8] whereas weight loss reduces AF risk.[47,48] These studies point to the causal association between obesity and AF pathogenesis. The molecular mechanisms underlying obesity-induced atrial arrhythmogenesis appears complex. Our data are the first to demonstrate that atrial NLRP3 inflammasome activity is required for obesity-induced AF arrhythmogenesis. We show that activity of the NLRP3 inflammasome is enhanced in atrial tissue of obese patients and in two animal models (i.e. sheep and mouse) of HFD-driven obesity. The lack of systematic inflammatory response in both human and mouse samples suggest that the local atrial tissue-specific enhancement of NLRP3 inflammasome activity drives AF in obesity.

The activation of the NLRP3 inflammasome requires two-steps known as 'priming' (transcription) and 'triggering' (assembly) processes.[20,21,49] Previous studies have shown that fatty acids can promote 'triggering' of the NLRP3 inflammasome via activation of ER stress in macrophages.[37] The molecular chaperone HSP5A (also known as the glucose-regulated protein of 78 kDa, GRP78) which normally resides near the ER, can act as a master controller of the unfolded protein response (UPR).[50] In macrophages, transcriptional upregulation of the NLRP3 inflammasome effector cytokines IL-1β and IL-18 is mediated through IRE1α (Inositol-Requiring Enzyme 1) upon dissociation of HSP5A.[51] Therefore, our results suggest that the increased expression and mobilization of HSP5A within atrial cardiomyocytes permits the transcription of UPR target genes, and drives NLRP3-inflammasome activity to promote inflammatory remodeling and AF development. Interestingly, the diet-induced increase in HSPA5 level was blunted by genetic deletion of NLRP3. This result points to a putative feedforward loop between NLRP3-inflammasome upregulation and ER-stress activation, which should amplify and spread atrial inflammatory signaling. However, whether the components or the effectors of NLRP3 inflammasome (e.g. Casp1 and IL-1β) are driving ER stress should be defined in future studies.

Previously, we have shown that the cardiomyocyte-specific activation of NLRP3 in a knock-in mouse model is sufficient to enhance AF inducibility via abbreviation of atrial refractoriness, a known substrate for AF.[23] Consistent with this report, increased NLRP3 expression in diet-induced obesity in mice was associated with shortened AERP, which was prevented by genetic NLRP3 inhibition. As in the mouse model with constitutive NLRP3 activation,[23] the expression of Kv1.5 channels was elevated in both atria of patients with increased BMI and mice with diet-induced obesity. The elevated Kv1.5 protein levels and the abbreviation of AERP in obese mice were corrected by NLRP3 inhibition. Thus, NLRP3 might directly regulate the transcription of *Kcna5*, which deems further detailed investigation.

Our observations in diet-induced obese mice are consistent with a recent report by McCauley *et al.*[11] that showed that WT mice with HFD challenge for 10 weeks exhibit APD shortening in atrial cardiomyocytes, slow conduction in left atrium, increased atrial fibrosis, and unchanged left atrial diameter. These authors also showed that both reduced function of Nav1.5 and Cav1.2 channels, and enhanced amplitude of Kv1.5 currents contribute to APD shortening, while we only observed an upregulation of Kv1.5 along with unchanged levels of Nav1.5 and Cav1.2 proteins in both obese mice and obese patients. Because we did not functionally analyse I_{Na}, $I_{Ca,\ L}$, and I_{Kur} with patch clamp, we cannot exclude a potential contribution of altered Nav1.5 and Cav1.2 function in our mouse model. In addition, CV was normal in RA of our obese mice, whereas McCauley *et al.*[11] detected a slowed CV in the left atrium of their obese mice. These different findings could result from chamber-specific effects of obesity, differences in employed methods for CV analysis or a combination of both. Subsequent work should directly address these possibilities.

Our study has limitations. The obese patients exhibit other comorbidities including diabetes and hypertension. Patients in the obesity group were treated with anti-diabetic medications and/or insulin. This should be considered when interpreting our human results. Due to technical challenges, we used the right atrial appendage from patients for biochemical analysis, and only analysed the AERP, CV, and APDs in RA of mice; therefore, this part of our results might not apply to the left atrium.

Although we observed abnormal SR Ca^{2+} leak in obesity, pointing to RyR2 dysfunction, the precise molecular mechanisms remain unclear. Proper control of protein phosphorylation is key for the function of cardiomyocyte proteins,[52] but phosphorylation level of 3 known serine sites on RyR2 was unchanged in obese mice. Thus, the precise molecular mechanisms of RyR2 dysfunction remain unclear and require further in-depth investigation. Several studies have suggested that obesity is associated with oxidative stress and increased reactive oxygen species (ROS) production which can directly modulate the function of CaMKII and RyR2.[11,53–55] Thus, the precise relationship between obesity, ROS, NLRP3-inflammasome activation, and AF should be addressed in follow-up studies with selective targeting of the different sources of ROS production. We used whole-body $NLRP3^{-/-}$ mice in our study, which may render compensatory or non-physiological changes; thus, our findings need validation with cardiac-restricted or atrial selective genetic manipulation of the NLRP3 inflammasome. In addition, previous work has provided evidence that NLRP3 could function as a transcription co-activator,[56] suggesting potential inflammatory signaling independent effects of NLRP3 that need further delineation in subsequent work. To determine the therapeutic anti-AF potential of NLRP3-inhibition in obesity, proper-controlled follow-up studies are required to establish the optimal duration, dose, window of opportunity, and administration route for a specific NLRP3-inhibitor (e.g. MCC950) in diet-induced obesity animal models as a pre-clinical study.

In conclusion, our study reveals that the NLRP3 inflammasome is an essential mechanistic link between obesity and atrial arrhythmogenesis. Our data suggest that selective inhibition of the NLRP3 inflammasome could prevent or reduce the risk of AF in obese patients who are unable to lose weight. The NLRP3 inflammasome might constitute a novel pharmacological approach for the prevention and treatment of AF patients.

Supplementary material

Supplementary material is available at *Cardiovascular Research* online.

Authors' contributions

N.L., L.S.J., and D.D. designed the study. L.S.J., A.C.F., A.S., L.L., D.L., X.C., X.W., J.L., M.H., D.T., T.T.P., R.D.L., and M.K. performed experiments and analysed results. N.L. and L.S.J. drafted the manuscript. M.G.C., M.L.E., G.E.T., P.S., D.D., and N.L. revised the manuscript for important intellectual content.

Acknowledgements

We thank the technical support from the Mouse Metabolic and Phenotyping Core at Baylor College of Medicine and the excellent technical assistance of Bettina Mausa. We thank Prof. Xander H.T. Wehrens at Baylor College of Medicine for providing intellectual discussions and antibodies for detecting the phosphorylated RyR2.

Conflict of interest: Dr Li's lab received research grant from BioIntervene Inc. for research activities outside the submitted work. Dr Dobrev is a member of the Scientific Advisory Boards of Omeicos Therapeutics GmbH and Acesion Pharma.

Funding

This study is supported by grants from National Institutes of Health [R01HL136389 to N.L. and D.D., R01HL147108 to N.L., and R01HL131517 and R01HL089598 to D.D.], American Heart Association [17PRE33660744 to L.S.J.], the European Union [large-scale network project MAESTRIA to D.D.], and the German Research Foundation [DFG, Do 769/4-1 to D.D.].

Data availability

The data underlying this article are available in the article and in its Supplementary material online.

References

1. Kornej J, Borschel CS, Benjamin EJ, Schnabel RB. Epidemiology of atrial fibrillation in the 21st century: novel methods and new insights. *Circ Res* 2020;**127**:4–20.
2. Rahman F, Kwan GF, Benjamin EJ. Global epidemiology of atrial fibrillation. *Nat Rev Cardiol* 2014;**11**:639–654.
3. Benjamin EJ, Chen PS, Bild DE, Mascette AM, Albert CM, Alonso A, Calkins H, Connolly SJ, Curtis AB, Darbar D, Ellinor PT, Go AS, Goldschlager NF, Heckbert SR, Jalife J, Kerr CR, Levy D, Lloyd-Jones DM, Massie BM, Nattel S, Olgin JE, Packer DL, Po SS, Tsang TS, Van Wagoner DR, Waldo AL, Wyse DG. Prevention of atrial fibrillation: report from a national heart, lung, and blood institute workshop. *Circulation* 2009;**119**:606–618.
4. Nattel S, Heijman J, Zhou L, Dobrev D. Molecular basis of atrial fibrillation pathophysiology and therapy: a translational perspective. *Circ Res* 2020;**127**:51–72.
5. Zimetbaum P. Antiarrhythmic drug therapy for atrial fibrillation. *Circulation* 2012;**125**:381–389.
6. Goudis CA, Korantzopoulos P, Ntalas IV, Kallergis EM, Ketikoglou DG. Obesity and atrial fibrillation: a comprehensive review of the pathophysiological mechanisms and links. *J Cardiol* 2015;**66**:361–369.
7. Guglin M, Maradia K, Chen R, Curtis AB. Relation of obesity to recurrence rate and burden of atrial fibrillation. *Am J Cardiol* 2011;**107**:579–582.
8. Tsang TS, Barnes ME, Miyasaka Y, Cha SS, Bailey KR, Verzosa GC, Seward JB, Gersh BJ. Obesity as a risk factor for the progression of paroxysmal to permanent atrial fibrillation: a longitudinal cohort study of 21 years. *Eur Heart J* 2008;**29**:2227–2233.
9. Chung MK, Eckhardt LL, Chen LY, Ahmed HM, Gopinathannair R, Joglar JA, Noseworthy PA, Pack QR, Sanders P, Trulock KM, American Heart Association E, Arrhythmias C, Exercise CR, Secondary Prevention Committee Of The Council On Clinical C, Council On Arteriosclerosis T, Vascular B, Council on C, Stroke N, Council on L, Cardiometabolic H. Lifestyle and risk factor modification for reduction of atrial fibrillation: a scientific statement from the American Heart Association. *Circulation* 2020;**141**:e750–e772.
10. Lau DH, Nattel S, Kalman JM, Sanders P. Modifiable risk factors and atrial fibrillation. *Circulation* 2017;**136**:583–596.
11. McCauley MD, Hong L, Sridhar A, Menon A, Perike S, Zhang M, da Silva IB, Yan J, Bonini MG, Ai X, Rehman J, Darbar D. Ion channel and structural remodeling in obesity-mediated atrial fibrillation. *Circ Arrhythm Electrophysiol* 2020;**13**:e008296.
12. Cheng T, Wang XF, Hou YT, Zhang L. Correlation between atrial fibrillation, serum amyloid protein A and other inflammatory cytokines. *Mol Med Rep* 2012;**6**:581–584.
13. Hu YF, Chen YJ, Lin YJ, Chen SA. Inflammation and the pathogenesis of atrial fibrillation. *Nat Rev Cardiol* 2015;**12**:230–243.
14. Wang H, Yan HM, Tang MX, Wang ZH, Zhong M, Zhang Y, Deng JT, Zhang W. Increased serum levels of microvesicles in nonvalvular atrial fibrillation determinated by ELISA using a specific monoclonal antibody AD-1. *Clin Chim Acta* 2010;**411**:1700–1704.
15. Luan Y, Guo Y, Li S, Yu B, Zhu S, Li S, Li N, Tian Z, Peng C, Cheng J, Li Q, Cui J, Tian Y. Interleukin-18 among atrial fibrillation patients in the absence of structural heart disease. *Europace* 2010;**12**:1713–1718.
16. Galea R, Cardillo MT, Caroli A, Marini MG, Sonnino C, Narducci ML, Biasucci LM. Inflammation and C-reactive protein in atrial fibrillation: cause or effect? *Tex Heart Inst J* 2014;**41**:461–468.
17. Zhang Y, Wang YT, Shan ZL, Guo HY, Guan Y, Yuan HT. Role of inflammation in the initiation and maintenance of atrial fibrillation and the protective effect of atorvastatin in a goat model of aseptic pericarditis. *Mol Med Rep* 2015;**11**:2615–2623.
18. Issac TT, Dokainish H, Lakkis NM. Role of inflammation in initiation and perpetuation of atrial fibrillation: a systematic review of the published data. *J Am Coll Cardiol* 2007;**50**:2021–2028.
19. Ozaki E, Campbell M, Doyle SL. Targeting the NLRP3 inflammasome in chronic inflammatory diseases: current perspectives. *J Inflamm Res* 2015;**8**:15–27.
20. Sutterwala FS, Haasken S, Cassel SL. Mechanism of NLRP3 inflammasome activation. *Ann NY Acad Sci* 2014;**1319**:82–95.
21. Elliott EI, Sutterwala FS. Initiation and perpetuation of NLRP3 inflammasome activation and assembly. *Immunol Rev* 2015;**265**:35–52.

22. Heijman J, Muna AP, Veleva T, Molina CE, Sutanto H, Tekook MA, Wang Q, Abu-Taha I, Gorka M, Kunzel S, El-Armouche A, Reichenspurner H, Kamler M, Nikolaev VO, Ravens U, Li N, Nattel S, Wehrens XH, Dobrev D. Atrial myocyte NLRP3/CaMKII nexus forms a substrate for post-operative atrial fibrillation. *Circ Res* 2020;**127**:1036–1055.
23. Yao C, Veleva T, Scott L, Cao S, Li L, Chen G, Jeyabal P, Pan X, Alsina KM, Abu-Taha I, Ghezelbash S, Reynolds CL, Shen YH, LeMaire SA, Schmitz W, Müller FU, El-Armouche A, Tony Eissa N, Beeton C, Nattel S, Wehrens XHT, Dobrev D, Li N. Enhanced cardiomyocyte NLRP3 inflammasome signaling promotes atrial fibrillation. *Circulation* 2018;**138**:2227–2242.
24. Li N, Brundel B. Inflammasomes and proteostasis novel molecular mechanisms associated with atrial fibrillation. *Circ Res* 2020;**127**:73–90.
25. Vandanmagsar B, Youm YH, Ravussin A, Galgani JE, Stadler K, Mynatt RL, Ravussin E, Stephens JM, Dixit VD. The NLRP3 inflammasome instigates obesity-induced inflammation and insulin resistance. *Nat Med* 2011;**17**:179–188.
26. Fender AC, Kleeschulte S, Stolte S, Leineweber K, Kamler M, Bode J, Li N, Dobrev D. Thrombin receptor PAR4 drives canonical NLRP3 inflammasome signaling in the heart. *Basic Res Cardiol* 2020;**115**:10.
27. Mahajan R, Lau DH, Brooks AG, Shipp NJ, Manavis J, Wood JP, Finnie JW, Samuel CS, Royce SG, Twomey DJ, Thanigaimani S, Kalman JM, Sanders P. Electrophysiological, electroanatomical, and structural remodeling of the atria as consequences of sustained obesity. *J Am Coll Cardiol* 2015;**66**:1–11.
28. NIH. *Guide for the Care and Use of Laboratory Animals*. 8th ed. Washington (DC): National Academies Press; 2011.
29. Brydges SD, Mueller JL, McGeough MD, Pena CA, Misaghi A, Gandhi C, Putnam CD, Boyle DL, Firestein GS, Horner AA, Soroosh P, Watford WT, O'Shea JJ, Kastner DL, Hoffman HM. Inflammasome-mediated disease animal models reveal roles for innate but not adaptive immunity. *Immunity* 2009;**30**:875–887.
30. Wang CY, Liao JK. A mouse model of diet-induced obesity and insulin resistance. *Methods Mol Biol* 2012;**821**:421–433.
31. Respress JL, Wehrens XH. Transthoracic echocardiography in mice. *J Vis Exp* 2010; e1738.
32. O'Shea C, Holmes AP, Yu TY, Winter J, Wells SP, Correia J, Boukens BJ, De Groot JR, Chu GS, Li X, Ng GA, Kirchhof P, Fabritz L, Rajpoot K, Pavlovic D. ElectroMap: high-throughput open-source software for analysis and mapping of cardiac electrophysiology. *Sci Rep* 2019;**9**:1389.
33. O'Shea C, Holmes AP, Yu TY, Winter J, Wells SP, Parker BA, Fobian D, Johnson DM, Correia J, Kirchhof P, Fabritz L, Rajpoot K, Pavlovic D. High-throughput analysis of optical mapping data using ElectroMap. *J Vis Exp* 2019;e59663.
34. Li N, Chiang DY, Wang S, Wang Q, Sun L, Voigt N, Respress JL, Ather S, Skapura DG, Jordan VK, Horrigan FT, Schmitz W, Muller FU, Valderrabano M, Nattel S, Dobrev D, Wehrens XHT. Ryanodine receptor-mediated calcium leak drives progressive development of an atrial fibrillation substrate in a transgenic mouse model. *Circulation* 2014;**129**:1276–1285.
35. Li N, Wang T, Wang W, Cutler MJ, Wang Q, Voigt N, Rosenbaum DS, Dobrev D, Wehrens XH. Inhibition of CaMKII phosphorylation of RyR2 prevents induction of atrial fibrillation in FKBP12.6 knockout mice. *Circ Res* 2012;**110**:465–470.
36. Picht E, Zima AV, Blatter LA, Bers DM. SparkMaster: automated calcium spark analysis with ImageJ. *Am J Physiol Cell Physiol* 2007;**293**:C1073–C1081.
37. Robblee MM, Kim CC, Porter Abate J, Valdearcos M, Sandlund KL, Shenoy MK, Volmer R, Iwawaki T, Koliwad SK. Saturated fatty acids engage an IRE1alpha-dependent pathway to activate the NLRP3 inflammasome in myeloid cells. *Cell Rep* 2016;**14**:2611–2623.
38. Quarti Trevano F, Dell'Oro R, Biffi A, Seravalle G, Corrao G, Mancia G, Grassi G. Sympathetic overdrive in the metabolic syndrome: meta-analysis of published studies. *J Hypertens* 2020;**38**:565–572.
39. Grassi G, Biffi A, Seravalle G, Trevano FQ, Dell'Oro R, Corrao G, Mancia G. Sympathetic neural overdrive in the obese and overweight state. *Hypertension* 2019; **74**:349–358.
40. Medrano G, Hermosillo-Rodriguez J, Pham T, Granillo A, Hartley CJ, Reddy A, Osuna PM, Entman ML, Taffet GE. Left atrial volume and pulmonary artery diameter are noninvasive measures of age-related diastolic dysfunction in mice. *Gerona* 2016; **71**:1141–1150.
41. Ujino K, Barnes ME, Cha SS, Langins AP, Bailey KR, Seward JB, Tsang TS. Two-dimensional echocardiographic methods for assessment of left atrial volume. *Am J Cardiol* 2006;**98**:1185–1188.
42. Dobrev D, Wehrens XHT. Calcium-mediated cellular triggered activity in atrial fibrillation. *J Physiol* 2017;**595**:4001–4008.
43. Vest JA, Wehrens XH, Reiken SR, Lehnart SE, Dobrev D, Chandra P, Danilo P, Ravens U, Rosen MR, Marks AR. Defective cardiac ryanodine receptor regulation during atrial fibrillation. *Circulation* 2005;**111**:2025–2032.
44. Campbell HM, Quick AP, Abu-Taha I, Chiang DY, Kramm CF, Word TA, Brandenburg S, Hulsurkar M, Alsina KM, Liu HB, Martin B, Uhlenkamp D, Moore OM, Lahiri SK, Corradini E, Kamler M, Heck AJR, Lehnart SE, Dobrev D, Wehrens XHT. Loss of SPEG inhibitory phosphorylation of ryanodine receptor type-2 promotes atrial fibrillation. *Circulation* 2020;**142**:1159–1172.
45. Middeldorp ME, Ariyaratnam J, Lau D, Sanders P. Lifestyle modifications for treatment of atrial fibrillation. *Heart* 2020;**106**:325–332.
46. Huang G, Parikh PB, Malhotra A, Gruberg L, Kort S. Relation of body mass index and gender to left atrial size and atrial fibrillation. *Am J Cardiol* 2017;**120**:218–222.
47. Pathak RK, Middeldorp ME, Meredith M, Mehta AB, Mahajan R, Wong CX, Twomey D, Elliott AD, Kalman JM, Abhayaratna WP, Lau DH, Sanders P. Long-term effect of goal-directed weight management in an atrial fibrillation cohort: a long-term follow-up study (LEGACY). *J Am Coll Cardiol* 2015;**65**:2159–2169.
48. Middeldorp ME, Pathak RK, Meredith M, Mehta AB, Elliott AD, Mahajan R, Twomey D, Gallagher C, Hendriks JML, Linz D, McEvoy RD, Abhayaratna WP, Kalman JM, Lau DH, Sanders P. PREVEntion and regReSsive effect of weight-loss and risk factor modification on atrial fibrillation: the REVERSE-AF study. *Europace* 2018;**20**: 1929–1935.
49. Toldo S, Mezzaroma E, McGeough MD, Pena CA, Marchetti C, Sonnino C, Van Tassell BW, Salloum FN, Voelkel NF, Hoffman HM, Abbate A. Independent roles of the priming and the triggering of the NLRP3 inflammasome in the heart. *Cardiovasc Res* 2015;**105**:203–212.
50. Kopp MC, Larburu N, Durairaj V, Adams CJ, Ali MMU. UPR proteins IRE1 and PERK switch BiP from chaperone to ER stress sensor. *Nat Struct Mol Biol* 2019;**26**: 1053–1062.
51. Tufanli O, Telkoparan Akillilar P, Acosta-Alvear D, Kocaturk B, Onat UI, Hamid SM, Cimen I, Walter P, Weber C, Erbay E. Targeting IRE1 with small molecules counteracts progression of atherosclerosis. *Proc Natl Acad Sci U S A* 2017;**114**:E1395–E1404.
52. Heijman J, Dewenter M, El-Armouche A, Dobrev D. Function and regulation of serine/threonine phosphatases in the healthy and diseased heart. *J Mol Cell Cardiol* 2013; **64**:90–98.
53. Hamilton S, Terentyeva R, Martin B, Perger F, Li J, Stepanov A, Bonilla IM, Knollmann BC, Radwański PB, Györke S, Belevych AE, Terentyev D. Increased RyR2 activity is exacerbated by calcium leak-induced mitochondrial ROS. *Basic Res Cardiol* 2020;**115**: 38.
54. Purohit A, Rokita AG, Guan X, Chen B, Koval OM, Voigt N, Neef S, Sowa T, Gao Z, Luczak ED, Stefansdottir H, Behunin AC, Li N, El-Accaoui RN, Yang B, Swaminathan PD, Weiss RM, Wehrens XH, Song LS, Dobrev D, Maier LS, Anderson ME. Oxidized Ca(2+)/calmodulin-dependent protein kinase II triggers atrial fibrillation. *Circulation* 2013;**128**:1748–1757.
55. Karam BS, Chavez-Moreno A, Koh W, Akar JG, Akar FG. Oxidative stress and inflammation as central mediators of atrial fibrillation in obesity and diabetes. *Cardiovasc Diabetol* 2017;**16**:120.
56. Bruchard M, Rebe C, Derangere V, Togbe D, Ryffel B, Boidot R, Humblin E, Hamman A, Chalmin F, Berger H, Chevriaux A, Limagne E, Apetoh L, Vegran F, Ghiringhelli F. The receptor NLRP3 is a transcriptional regulator of TH2 differentiation. *Nat Immunol* 2015;**16**:859–870.

Translational perspective

Obesity and inflammation are two well-established risk factors of atrial fibrillation (AF). Our study is the first to establish that NLRP3 inflammasome—an innate inflammatory signaling—is a nodal signal mediating the atrial arrhythmogenesis in the context of obesity. Inhibition of NLRP3 inflammasome prevents the obesity-induced development of ectopic activity and a reentry substrate for AF in mice. Our study provides a proof-of-concept that targeting the NLRP3 inflammasome or its downstream effectors (e.g. caspase-1, IL-1β) may be beneficial for AF-prevention in obese patients.